Test of the optical theory of Mössbauer quantum beats

E. H. du Marchie van Voorthuysen, G. L. Zhang,* and H. de Waard
Laboratorium voor Algemene Natuurkunde, Rijksuniversiteit Groningen, Groningen, The Netherlands
(Received 1 June 1984)

Quantum-beat and sideband spectra of recoilless γ radiation of ^{57}Fe were measured as a function of frequency and the voltage on the quartz crystal on which a ^{57}Co source was deposited. The sideband spectra were analyzed using a Rice distribution of the modulation index. The width of this distribution was shown to depend on the frequency; the narrowest distribution was found at 9.795 MHz. The results of the quantum-beat measurements are in agreement with the optical theory of Monahan and Perlow.

I. INTRODUCTION

When a source of recoillessly emitted γ rays is vibrated at a high frequency and the emitting nuclei make several oscillations on the average during their decay, the frequency modulation of the γ rays becomes visible in the energy spectrum. Sidebands appear in this spectrum as it is measured by slowly moving a resonant absorber between source and detector. Sideband spectra were observed for the first time by Ruby and Bolef.[1] One may understand the sidebands as the result of the interaction between γ quanta and ultrasonic phonons.[2] From a sideband spectrum the intensity and the frequency of the phonons can be obtained. The phase of the phonons does not play any role and perfect sideband specta can be measured with sources with thickness larger than the ultrasonic wavelength.[3]

The phase of the phonons can be determined in a quantum-beat measurement.[4,5] The absorber is at rest with respect to the source (or moves at a constant velocity), and the arrival time of the γ rays is measured with respect to the phase of the rf signal that drives the source. Beats occur in the obtained time spectrum due to the interference between the sidebands or between one sideband and the carrier. In order to be able to observe quantum beats, phase changes of the source vibration must be kept small during the several hours needed to measure a spectrum as well as the phase spread over the area of the source (several millimeters). The thickness of the source must be small with respect to the ultrasonic wavelength.

A theoretical description of the quantum-beat spectra has been given by Monahan and Perlow.[5] A quantum-beat spectrum measured with a ^{67}Zn source at a frequency of 65 kHz was in accordance with the theory.[6] The other quantum-beat measurements reported until now[3-5,7] were performed with ^{57}Co and ^{129m}Te sources at frequencies of 10 and 30 MHz, respectively. The Monahan theory was tested to a limited extent,[3,7] but in all cases the amplitudes of the beat components in the measured spectra were smaller than the theoretical values. So the sources were not completely coherent, if we assume that the theory of Monahan is correct.

Only in a few cases[8-10] is the intensity of the sidebands in reasonable accordance with the simple $J_n^2(a)$ behavior [see Eq. (4), Sec. II], in which it is assumed that the vibration amplitudes of all nuclei are equal. In all other cases, the intensity of the sidebands is proportional to $\exp(-a_R^2)I_n(a_R^2)$ [see Eq. (9), Sec. II]; see, for instance, Refs. 2, 3, and 11. This result is in accordance with a Rayleigh distribution for the amplitude of the vibration source nuclei. In the literature such a source is often called incoherent. This is confusing, because it would be impossible to observe quantum beats from a really incoherent source, in contrast to reality.[3,5,7] Therefore, it is better to introduce a degree of coherence that is related to the observed quantum-beat structure.

II. THEORETICAL SUMMARY

The electric field vector of the γ radiation from a decaying state with mean lifetime $1/\lambda$, measured at a distance $x-x_s$ from the source, is

$$E(x,t,t_0)=\begin{cases}\lambda^{1/2}\exp\left[-\frac{1}{2}\lambda(t-t_0)+i\left[\omega_0 t-\dfrac{x-x_s}{\lambda\!\!\!^{-}}\right]\right] & \text{for } t\geq t_0\\ 0 \text{ for } t<t_0\end{cases} \tag{1}$$

where t_0 is the formation time of the state, ω_0 the angular frequency of the γ ray, and $\lambda\!\!\!^{-}$ the reduced wavelength.

The source vibrates harmonically:

$$x_s=x_c+x_0\sin(\Omega t)\ . \tag{2}$$

After substitution into Eq. (1) and neglecting a constant phase we find

$$E(t,t_0)=\begin{cases}\lambda^{1/2}\{-\frac{1}{2}\lambda(t-t_0)+i[\omega_0 t+a\sin(\Omega t)]\} & \text{for } t\geq t_0\\ 0 \text{ for } t<t_0\end{cases} \tag{3}$$

with $a=x_0/\lambda$, the modulation index, which is proportional to the vibration amplitude.

A. The sideband spectrum

The frequency spectrum of phase-modulated γ rays is found by Fourier transforming Eq. (3), squaring the modulus, and integrating over all formation times t_0. The result[1,5] (except for a proportionality constant) is

$$I(\omega)=\sum_{n=-\infty}^{\infty}\frac{J_n^2(a)}{(\omega-\omega_0+n\Omega)^2+\frac{1}{4}\lambda^2}, \tag{4}$$

where J_n is the Bessel function of the first kind of order n. The same result can be obtained by a quantum-mechanical treatment.[2,12]

Most observed sideband spectra can be described very well[2,3,11] with the formula

$$I(\omega)=\sum_{n=-\infty}^{\infty}\frac{\exp(-\frac{1}{2}\langle a^2\rangle)I_n(\frac{1}{2}\langle a^2\rangle)}{(\omega-\omega_0+n\Omega)^2+\frac{1}{4}\lambda^2}, \tag{5}$$

where I_n is the modified Bessel function of the first kind of order n. This formula can be derived in several ways.

(i) Quantum mechanically, assuming an incoherent distribution of the ultrasonic phonons (Abragam,[13] Mishory and Bolef[2]). Mishory and Bolef justified this by assuming that the ultrasonic phonon-relaxation time is very short. This, however, is not true for crystals vibrating in their lowest-frequency vibration modes.[14]

(ii) Classically, assuming phase incoherence[13] (i.e., a uniform distribution of phases). However, since quantum-beat spectra are observed for sources which exhibit sideband spectra according to Eq. (5), this assumption cannot be true.[3]

(iii) Quantum mechanically, assuming a finite coherence time τ_c which is larger than the nuclear lifetime $1/\lambda$ but smaller than the total time needed for the measurement (Gupta[15]). This is the same assumption as that which underlies (ii).

(iv) Quantum mechanically, assuming a Rayleigh distribution of the number of phonons in the ultrasonic mode, but not specifying anything about phases (Pfeiffer *et al.*[12]). We think that the approach of Pfeiffer *et al.* is correct.

We will now formulate the problem in classical terms. γ rays are emitted by a large number of nuclei, vibrating with the same frequency but with different amplitudes and phases

$$x_i(t)=a_i\lambda\sin(\Omega t+\alpha_i). \tag{6}$$

The sideband spectrum from each nucleus is given separately by Eq. (4). When the amplitudes of the nuclei are distributed with a probability function $P(a)$, we must weigh Eq. (4) with this probability function:

$$I(\omega)=\sum_{n=-\infty}^{\infty}\int_{-\infty}^{\infty}\frac{P(a)J_n^2(a)da}{(\omega-\omega_0+n\Omega)^2+\frac{1}{4}\lambda^2}. \tag{7}$$

If we assume that the probability function for the amplitudes is a Rayleigh distribution

$$P(a)=\frac{a}{a_R^2}\exp\left[-\frac{a^2}{2a_R^2}\right] \tag{8}$$

the sideband spectrum becomes[16]

$$I(\omega)=\sum_{n=-\infty}^{\infty}\frac{\exp(-a_R^2)I_n(a_R^2)}{(\omega-\omega_0+n\Omega)^2+\frac{1}{4}\lambda^2}, \tag{9}$$

which is equal to Eq. (5) because for a Rayleigh distribution $\langle a^2\rangle=2a_R^2$.

The phase of the vibration is irrelevant in this argument. There may be a distribution of phases ranging from a uniform one to a δ function, and the phase distribution may be correlated with the amplitude distribution or not.

The assumption that the distribution of the amplitudes is a Rayleigh distribution is an *ad hoc* assumption, which is justified by the fact that it is a simple distribution function for a variable that can take only positive values and that many experimental sideband spectra agree with Eqs. (5) or (9). In these cases, the vibrational energy of the source is probably shared by many modes. The component of the vibration amplitude in the direction of the γ-ray detector may therefore vary as a function of the position of the emitters on the source or as a function of time.

In general the width of the amplitude distribution may be smaller than that of a Rayleigh distribution. A good choice is then the Rice distribution:[17,18]

$$P(a)=\frac{a}{a_R^2}I_0\left[\frac{aa_c}{a_R^2}\right]\exp\left[-\frac{a^2+a_c^2}{2a_R^2}\right]. \tag{10}$$

In the limit $a_c\to 0$ the Rice distribution is equal to the Rayleigh distribution. For $R=a_c/a_R\gg 1$ we find an average value for a, $\langle a\rangle\cong a_c$ and a standard deviation $\cong a_R$. We will call R the amplitude sharpness of the source. For $a_R\to 0$ we get the delta function $\delta(a-a_c)$.

B. The quantum-beat spectrum

Monahan and Perlow[5] derived the following formula for the quantum-beat spectrum, using classical optical theory:

$$I(t)=1+\sum_{n=-\infty}^{\infty}\sum_{l=-\infty}^{\infty}J_n(a)J_l(a)G_{nl}(\Delta\omega)\times\exp[i(n-l)\Omega t]. \tag{11}$$

The complex function G_{nl} is given by Eq. (2.16') in Ref. 5 and depends on the isomer shift $\Delta\omega$ between source and absorber, the thickness of the absorber, the vibration frequency Ω, the natural linewidth λ, and the width λ' of a Lorentzian distribution of isomer shifts in source and/or absorber. We assume a distribution of modulation index $P(a)$ and a distribution of phases that are uncorrelated. The effect of the phase distribution is an attenuation of the amplitudes of the beat components in the quantum-beat spectrum F_j. When the phase distribution is Gaussian with standard deviation σ, the attenuation coefficients are[5]

$$F_j=\exp[-\tfrac{1}{2}(j\sigma)^2] . \tag{12}$$

We define the degree of coherence C as follows:

$$C=\frac{1}{n}\sum_{j=1}^{n} F_j , \tag{13}$$

where the summation is made for the most relevant components.

We rewrite (11) as

$$I(t,a_c,a_R,\Delta\omega)=1+D_0(a_c,a_R,\Delta\omega)+\sum_{j=1}^{\infty}2\,|\,D_j(a_c,a_R,\Delta\omega)\,|\times\cos[j\Omega t+\phi_j(a_c,a_R,\Delta\omega)] \tag{14}$$

with

$$D_j(a_c,a_R,\Delta\omega)=\sum_{l=-\infty}^{\infty}\left[\int_0^{\infty}P(a,a_c,a_R)J_{j+l}(a)J_l(a)da\right]\times F_jG_{j+l\,l}(\Delta\omega)$$

and

$$\phi_j(a_c,a_R,\Delta\omega)=\arg D_j(a_c,a_R,\Delta\omega) .$$

The spectrum consists of a constant background and a series of beat components with frequencies equal to the vibration frequency and its harmonics. If the time is not measured we must average Eq. (14) over t and we find a constant $1+D_0(a_c,a_R,\Delta\omega)$. The term $D_0(a_c,a_R,\Delta\omega)$ is a real negative number which describes the resonant absorption. In a normal Mössbauer transmission experiment, $\Delta\omega$ is artifically varied by means of the Doppler effect, and for $\langle a\rangle\neq 0$ we find the sideband spectrum.

III. MEASUREMENTS AND CALCULATIONS

A 0.3-mm-thick X-cut quartz crystal was covered on both sides with a 1.0- and a 0.3-μm-thick copper electrode. Into the thick electrode 112-keV ^{57}Co ions were implanted up to a source strength of 5 μCi; see Fig. 1. No annealing was done. The linewidth, measured with a thin ^{57}FeRh absorber, was 0.30 mm/s. All measurements were

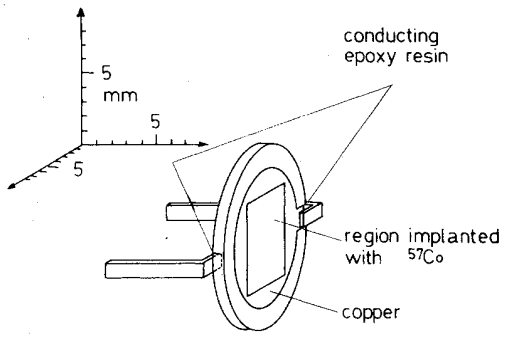

FIG. 1. Mounting of the source.

done with a thick $Na_4{}^{57}Fe(CN)_6\cdot 10H_2O$ absorber ($t_a=6.4$). The isomer shift with respect to ^{57}CoCu is $-0.2919(7)$ mm/s (Ref. 19). The γ rays were detected with a 0.1-mm-thick NaI(Tl) crystal. The block diagram is given in Fig. 2. The time-to-amplitude converter (TAC) is started by the fast signal from the detector. A signal that has a constant phase with respect to the driving electric field in the piezoelectric crystal stops the TAC. Only one out of eight pulses is admitted, enabling the observation of eight periods in the time spectra.

The output pulses from the linear gate were processed in two different ways. (1) During the quantum-beat measurements the absorber was at rest and the digital information from the analog-to-digital converter (ADC) was processed by the multichannel counter (MCC) interface.[20] (2) During the sideband measurements the absorber was moving at constant acceleration and all pulses were counted as a function of velocity.

The time resolution of the system was determined by measuring the γ—x-ray coincidences from a ^{88}Y source with the help of an extra plastic scintillation detector, which is connected to the system at the point in the block diagram indicated by V_t. The full width at half maximum of the measured prompt time peak was 8.4 ns. With the aid of the measured time spectrum attenuation factors T_j were calculated numerically for each harmonic component in the quantum-beat spectrum. The results are $T_1=0.879$, $T_2=0.682$, $T_3=0.529$, and $T_4=0.422$. The dependence of these numbers on the frequency will be neglected in Sec. III B.

The quantum-beat spectra were analyzed with the function

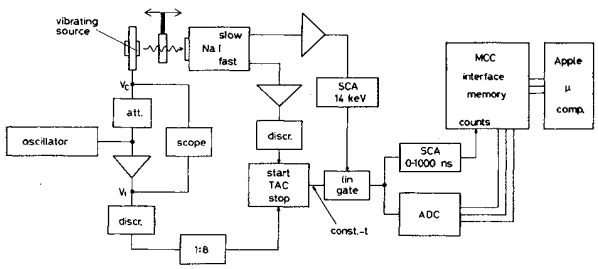

FIG. 2. Block diagram.

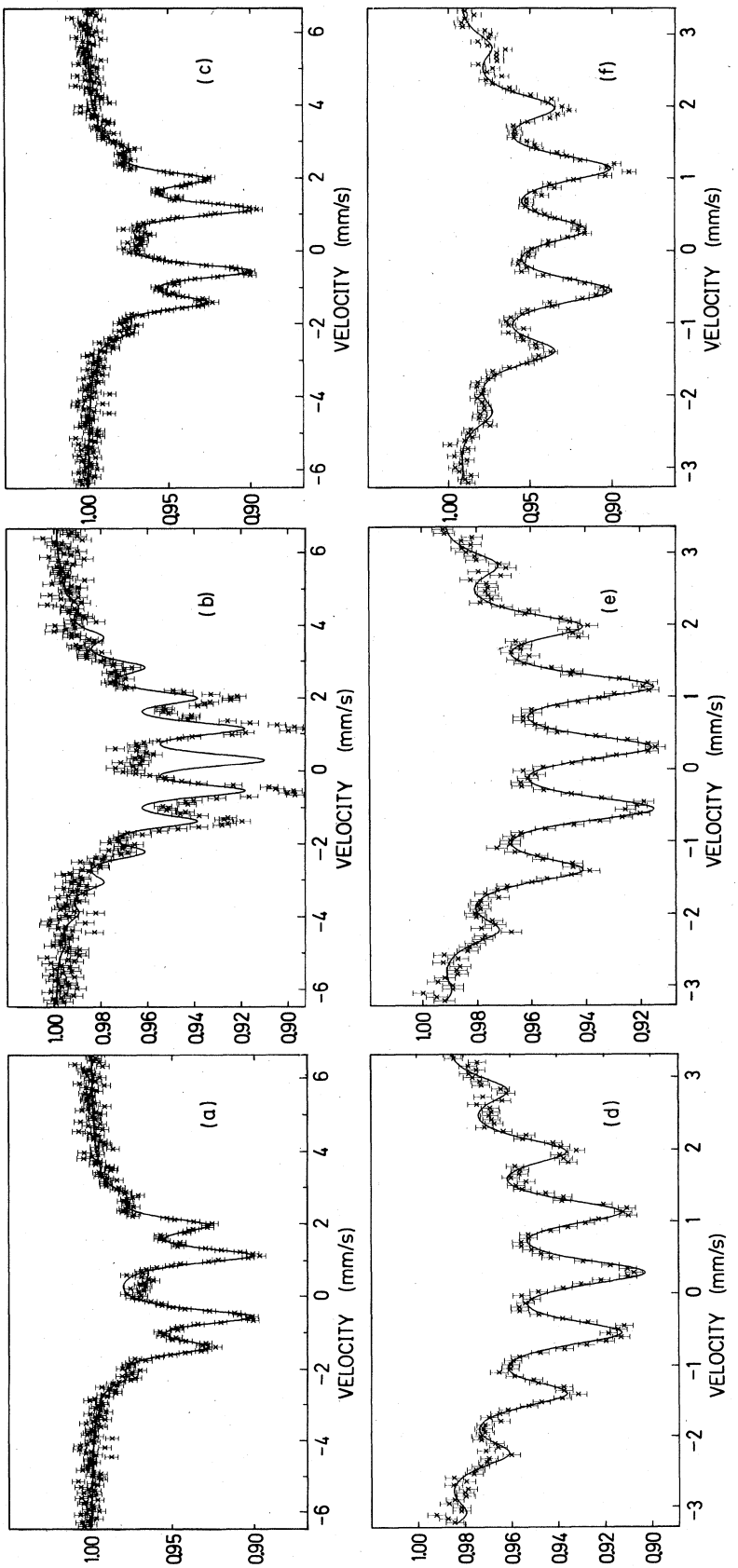

FIG. 3. Sideband spectra for three different rf frequencies and constant average modulation index. (a) 9.795 MHz, solid curve: Eq. (4), $\chi^2=1.55$, $a=2.39(2)$; (b) same spectrum, solid curve: Eq. (9), $\chi^2=11.1$, $a_R=2.3(1)$; (c) same spectrum, solid curve: Eqs. (7) and (10), $\chi^2=1.24$, $a_c=2.36(2)$, $a_R=0.40(3)$; (d) 9.755 MHz, solid curve: Eq. (9), $\chi^2=1.23$, $a_R=2.202(8)$; (e) same spectrum, solid curve: Eqs. (7) and (10), $\chi^2=0.98$, $a_c=1.95(4)$, $a_R=1.18(5)$; (f) 9.80625 MHz, solid curve: Eqs. (7) and (10), $\chi^2=1.07$ $a_c=1.99(3)$, $a_R=0.94(3)$.

$$I(t')=C'\left[1+\sum_{j=1}^{4} A_j\cos(j\Omega t'+P_j)\right] \tag{15}$$

with C', A_j, and P_j as free parameters. The experimental amplitudes are reduced with respect to the theoretical amplitudes $2\,|\,D_j\,|$ for two reasons. (1) Only a fraction f of the photons is recoillessly emitted, and (2) the oscillations are attenuated due to the finite time resolution of the detection system. Taking these effects into account, we find from Eqs. (14) and (15)

$$A_j=\frac{2fT_j\,|\,D_j\,|}{1+fD_0}\ . \tag{16}$$

The shape of the Mössbauer spectrum becomes

$$I(a_c,a_R,\Delta\omega)=1+fD_0(a_c,a_R,\Delta\omega)\ , \tag{17}$$

where $\Delta\omega$ is artifically varied by means of the Doppler effect.

The time scale in Eq. (14) was chosen such that at $t=0$ the source is at equilibrium position. The laboratory time scale t' differs from t:

$$t=-t'+\frac{\alpha}{\Omega}+\frac{\beta}{\Omega}+\Delta t\ , \tag{18}$$

in which α is the phase of the mechanical vibration of the source with respect to the phase of the electric field acting on the piezoelectric crystal, β the phase of V_c with respect to V_t (Fig. 2), and Δt an unknown electronic time delay which is assumed to be constant throughout the measurement. From Eqs. (14), (15), and (18) we find for the corrected phases of the components in the quantum-beat spectrum:

$$P_{j\,\mathrm{corr}}=P_j+j\beta=-\phi_j-j(\alpha+\Omega\Delta t)+n_j2\pi \qquad (n_j \text{ integer}) \tag{19}$$

or

$$\alpha=-\left[\frac{P_j+\phi_j}{j}+\beta+\Omega\Delta t\right]+\frac{n_j2\pi}{j}\ . \tag{20}$$

The sideband spectra were analyzed with Eqs. (7) and (10), using the following free parameters: the Rice parameters a_c and a_R, the intensity of the absorption integral, the isomer shift, the distance between the sidebands Ω, and the effective width of the separate lines. From a_c and a_R the average value of the modulation index and the amplitude sharpness $R=a_c/a_R$ was calculated.

A. Sideband spectra as a function of rf frequency

On the basis of a preliminary measurement the voltage of the rf signal, V_c, was chosen to correspond to an average value of the modulation index of about 2.4. For this value, the central line (carrier) in the sideband spectrum disappears in the case of a delta function, $P(a)=\delta(a-a')$ for the modulation index ($R=\infty$), so the sensitivity for the determination of the amplitude sharpness R is large. In Fig. 3 sideband spectra are shown for three different rf frequencies and $\langle a\rangle=2.2$–2.4. In all cases the best least-squares fits are obtained for a Rice distribution of modulation indices. The R is strongly dependent on the frequency, its maximum value lies at 9.795 MHz, where the intensity of the carrier is still significantly larger than it would have been for a unique value of the modulation index [Fig. 3(a)]. In Fig. 4 Rice distribution functions $P(a)$ of the modulation index are drawn [Eq. (10)], using the parameters a_c and a_R as they are determined from the least-squares fits to the spectra.

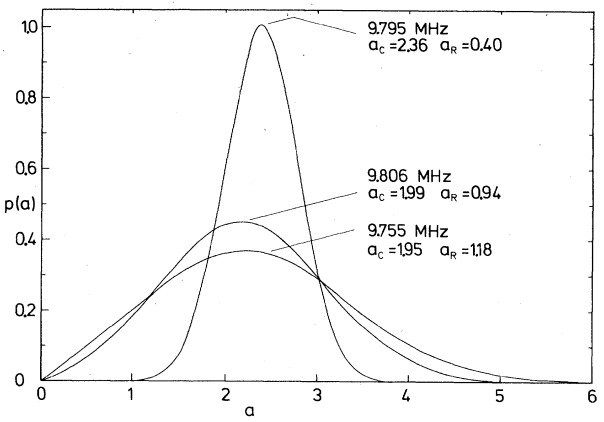

FIG. 4. Distribution function of the modulation index for the same rf frequencies as in Fig. 3.

The results of the measurements are summarized by Fig. 5. The resonance curve $\langle a\rangle/V_c$ has a complicated shape, indicating that there exist many vibration modes between 9.7 and 9.9 MHz. The maximum vibration amplitude occurs at 9.8075 MHz. An interesting feature is

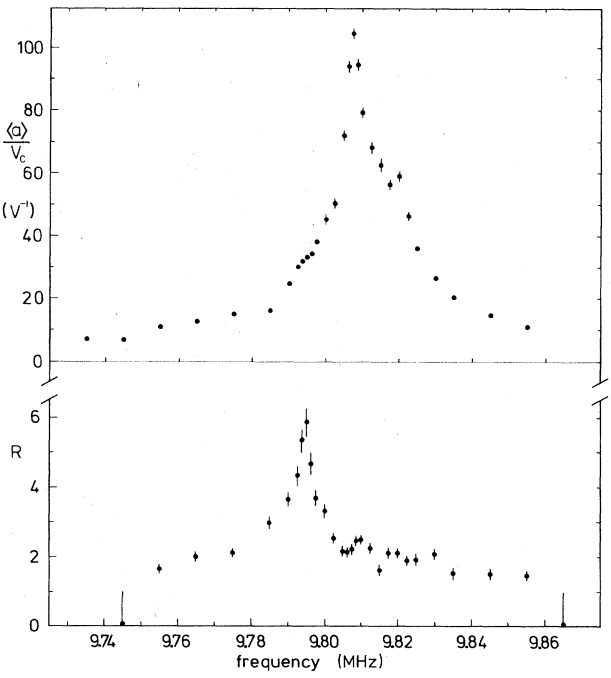

FIG. 5. Resonance curve of the source (top), amplitude sharpness as a function of frequency (bottom).

the behavior of the amplitude sharpness R as a function of frequency. This function has a sharp maximum at 9.795 MHz, at which frequency we find only a small shoulder in the resonance curve. The top of the resonance curve is at a much higher frequency.

B. Quantum-beat spectra as a function of rf frequency

The value V_c of the driving rf voltage was chosen such that the average modulation index $\langle a \rangle$ was equal to 1. At this value the amplitude of the fundamental component A_1 has its maximum value (see Fig. 11). The proportionality between V_c and $\langle a \rangle$ was checked in Sec. III C.

Figure 6 gives a quantum-beat spectrum at 9.795 MHz and $\langle a \rangle = 1.00$. The spectrum was analyzed with Eq. (15) with the following results: $A_1 = 0.278(1)$, $A_2 = 0.054(1)$, $P_1 = 3.209(5)$ rad, and $P_2 = 5.77(2)$ rad.

The theoretical amplitudes and phases were calculated with the Monahan theory [Eqs. (10), (14), and (16) for $F_j = 1$]. The width parameter λ' which is necessary to calculate the coefficients G_{nl} was fixed at the value where $D_0(0,0,\Delta\omega)$, calculated as a function of $\Delta\omega$, has the same shape as the Mössbauer dip of the nonvibrating source: $\lambda' = 0.152$ mm/s. An effective recoilless fraction $f = 0.642$ of the source was determined from the Mössbauer absorption maximum, the theoretical value of $D(0,0,0)$, and Eq. (17). The theoretical amplitudes are $A_1 = 0.298$ and $A_2 = 0.060$. A comparison with the experimental values shows that the source is not completely coherent. The theoretical phases are: $\phi_1 = -1.276$ and $\phi_2 = -1.878$ rad. According to Eq. (20) $x = (P_j + \phi_j)/j$ should be independent of j. We find $x = 1.933(5)$ for $j = 1$ and $x = 1.944(10)$ for $j = 2$, values which are in good agreement.

The results of the measurement are summarized in Fig. 7. The structure in the curves giving the theoretical amplitudes is caused by the variation of the amplitude sharpness R with frequency (Fig. 5). The degree of coherence of the source has a maximum value in the frequency range where the amplitude sharpness has a peak, although the coherence peak is much broader. So there seems to be a correlation between the amplitude sharpness and the degree of coherence.

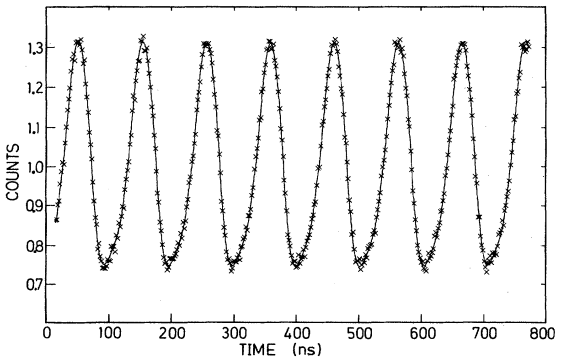

FIG. 6. Quantum-beat spectrum, solid curve: fit using Eq. (15) with $C' = 1$.

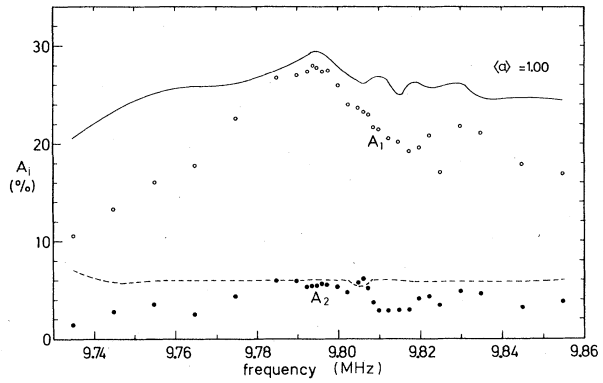

FIG. 7. Experimental and theoretical amplitudes of quantum beats as a function of frequency. Solid curve, theoretical A_1; dashed curve, theoretical A_2. No distribution of phases was assumed.

The phase difference α of the mechanical vibration of the source and the driving field was calculated (except for a constant) with Eq. (20) (see Fig. 8). The phase jump over the whole region is π, as it should be with a mechanical vibrator. We see a nice correlation between phase and amplitude: where the phase decreases most rapidly with frequency we find peaks or shoulders in the resonance curve.

C. Sideband spectra as a function of rf voltage

The measurements were performed at 9.795 MHz, where the amplitude sharpness R has its maximum value. The spectra were analyzed with a Rice distribution of modulation indices. The amplitude sharpness turned out to be constant for $\langle a \rangle > 1.5$. For lower values of $\langle a \rangle$ the error in R became too large, and the R was kept constant in the least-squares fits to the spectra. The modulation-

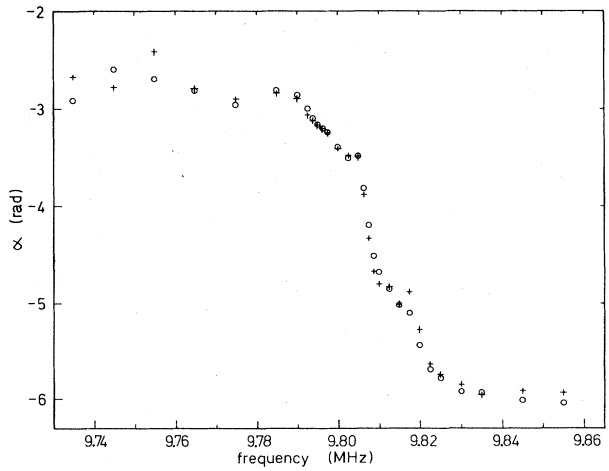

FIG. 8. Phase of the source vibration with respect to the driving rf signal. Circles, derived from the fundamental frequency ($j = 1$); crosses, derived from the second harmonic ($j = 2$).

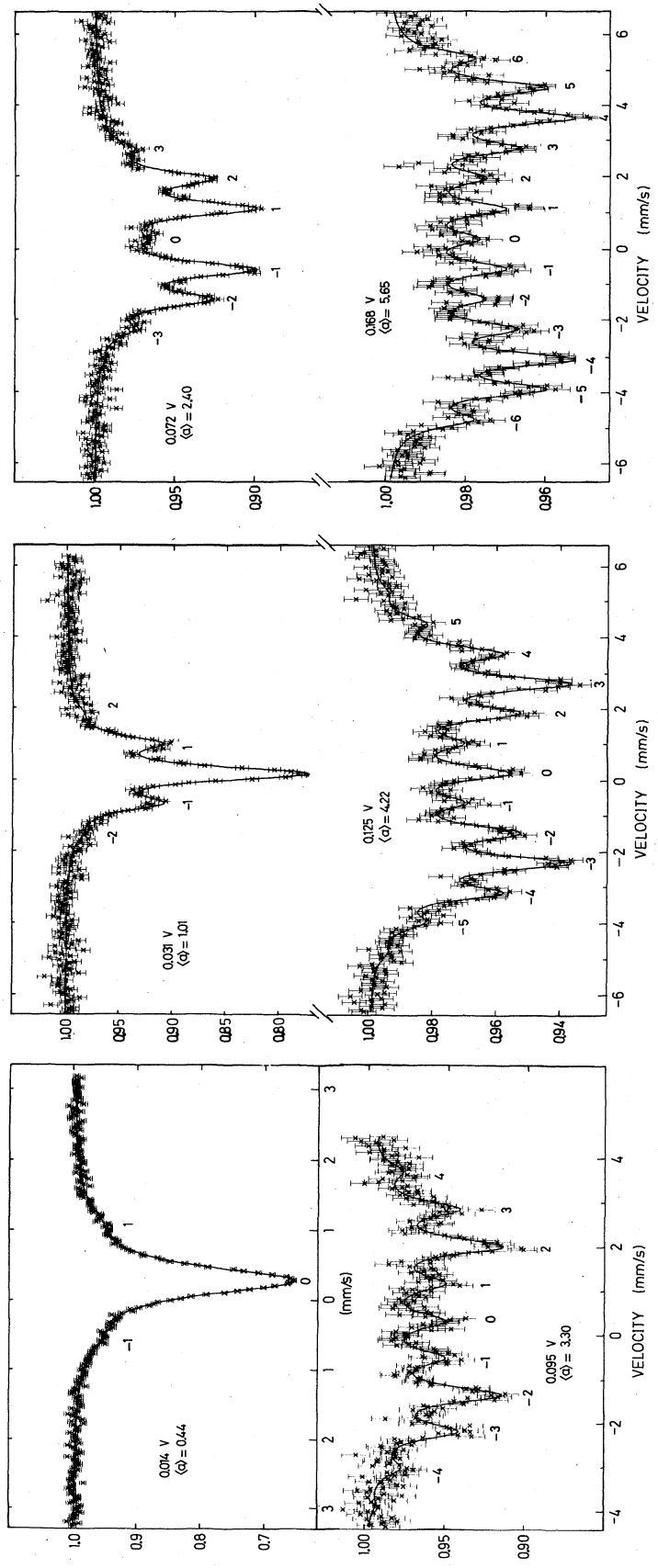

FIG. 9. Sideband spectra as a function of rf voltage. The spectra are labeled with the effective value of the voltage and the average value of the modulation index, which is a result of the fits using Eqs. (7) and (10) (solid curves). The separate sidebands are indicated with their index n [Eq. (7)].

index parameters a_c and a_R turn out to be proportional to the rf voltage V_c. A few spectra are given in Fig. 9. The oscillating behavior of the carrier and the lowest order ($|n|<4$) sidebands can be clearly seen.

D. Quantum-beat spectra as a function of rf voltage

The measurements were performed at 9.795 MHz. A few spectra are given by Fig. 10. At a small modulation index the only frequency in the quantum-beat spectrum is the fundamental frequency. In fact, the spectrum gives a direct projection of the movement of the source. From the shape of the spectra at a small modulation index we conclude that the movement is harmonic. It is much more difficult to draw such a conclusion from measured sideband spectra.[21] In Fig. 10 we see that the second harmonic contribution is growing between $\langle a\rangle=1.5$ and 2.5. At $\langle a\rangle=5.8$ the higher harmonics are clearly visible.

The measurements are summarized in Figs. 11–13. The theoretical curves were calculated with Eqs. (16), (14), and (10) with $R=5.89$ and $F_j=1$. No parameter was adjusted to the experimental amplitudes. The oscillations in the theoretical amplitudes are very well reproduced by the experiment, although the peak-to-valley ratio of the experimental points seems to be reduced with respect to the theory. Possibly, the width of the distribution of modulation indices is still somewhat larger than the width of a Rice distribution with $R=5.89$.

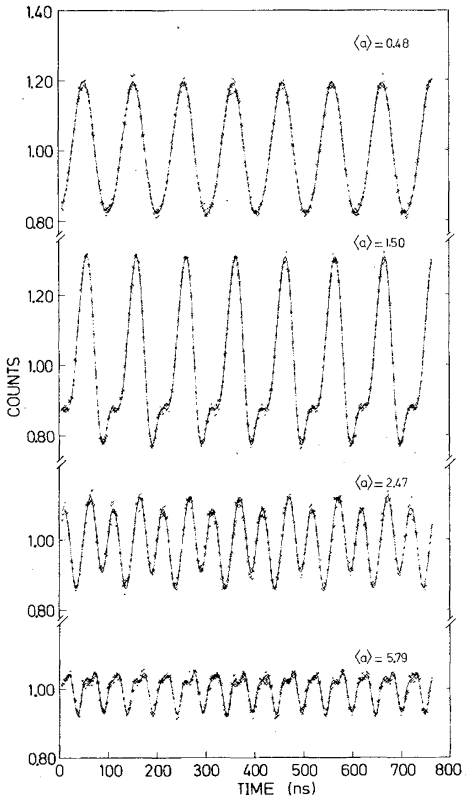

FIG. 10. Quantum-beat spectra as a function of rf voltage. Solid curves: fits using Eq. (15) with $C'=1$. Spectra are labeled with the average value of the modulation index as it is determined in Sec. III C.

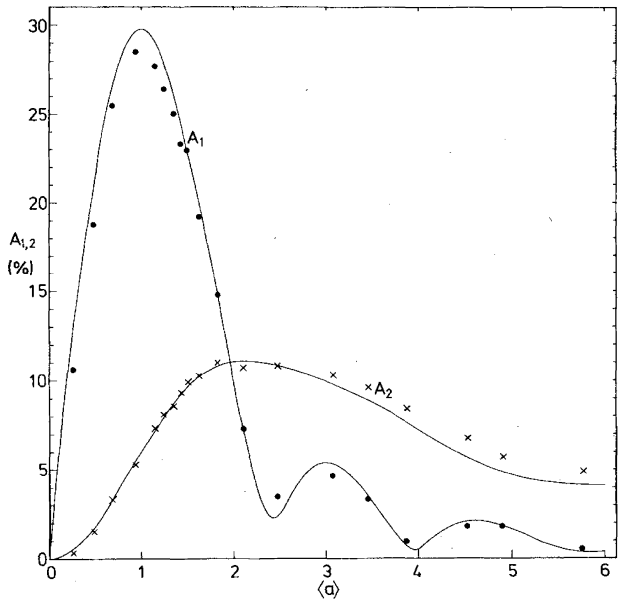

FIG. 11. Amplitudes of the 9.795- and 19.59-MHz components in the quantum-beat spectra as a function of modulation index. The statistical errors are smaller than the points. Solid curves are results of calculations (see text).

The experimental A_3 and A_4 values are systematically smaller than the theoretical values. Of course, we obtain a better agreement when the attenuation factors F_j are free parameters in a least-squares fit of the amplitudes. The results are $F_1=0.955(7)$, $F_2=1.033(12)$, F_3

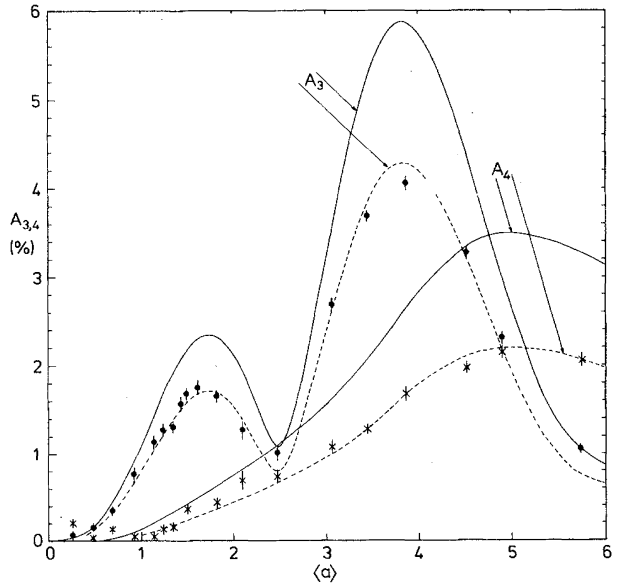

FIG. 12. Amplitudes of the 29.385 and 39.18-MHz components in the quantum-beat spectra as a function of modulation index. Solid curves are results of calculations, dashed curves are results of fits with F_3 and F_4 as free parameters.

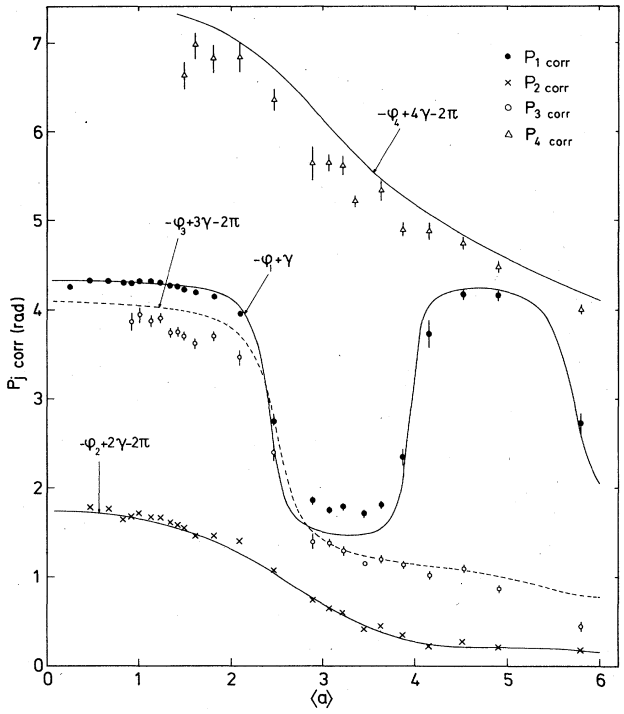

FIG. 13. Corrected phases of the components in the quantum-beat spectra as a function of modulation index. The curves are the result of one fit with γ as a free parameter.

$=0.729(11)$, and $F_4=0.628(12)$. The degree of coherence [Eq. (13)] calculated from the first and second harmonic is $C_{12}=0.97$ and calculated from all components $C_{14}=0.87$.

The phases of the components in the quantum-beat spectra, corrected for the phase angle β between V_c and V_t, are plotted in Fig. 13. All points were fitted simultaneously to Eq. (19) [and Eqs. (10) and (14)] with $\gamma=-\alpha-\Omega\Delta t$ as the only free parameter. The agreement between experiment and theory is good, except for a small reduction of the peak-to-valley ratio $P_{1\,\mathrm{corr}}$ and a shift of about 0.3 rad for $P_{4\,\mathrm{corr}}$.

IV. DISCUSSION

The high-frequency properties of the source can be summarized as follows. At the optimum frequency, 9.795 MHz, the amplitude sharpness is $R=5.9$ (which means a relative FWHM of the modulation-index distribution of 30%, see Fig. 4). The degree of coherence for the first and second harmonics is 97%. The quantity of this source is much better than any other high-frequency source reported up to now. This is probably caused by the mounting of the crystal, which is the same as the mounting of commercial AT-cut crystals used for frequency control, and the method which is applied to attach the radioactive material to the quartz crystal. In our earlier work[7] the crystal was mounted in the same way, but a diffusion process at 900 °C was necessary, which probably spoiled the crystal.

A thorough test was made of the optical theory of Monahan and Perlow. When we restrict ourselves for the moment to the first and second harmonics in the quantum-beat spectra, the amplitudes are correctly reproduced by the theory within an accuracy of 5%. The phases are reproduced very well, with the electronic delay at Δt as the only free parameter for the whole measurement. At extreme values of the amplitudes and phases there is a discrepancy between theory and experiment. We think that it is caused by a variation in modulation indices which is somewhat larger than the variation according to the Rice distribution. Although the Rice distribution is an elegant way to describe the distribution function of the modulation indices, it is only a model which works reasonably for the description of sideband spectra, but may deviate from reality. So the discrepancy at the extreme values is probably no indication of failure of the theory.

The large attenuation factors for the third and fourth harmonics do not allow a statement about the validity of the theory concerning these harmonics, although the phases are in reasonable agreement with the theory.

ACKNOWLEDGMENTS

One of us (G.L.Z.) gratefully acknowledges the warm hospitality at the Laboratorium voor Algemene Natuurkunde. This work was performed as part of the research program of the Stichting voor Fundamenteel Onderzoek der Materie (FOM) with financial support from the Nederlandse Organisatie voor Zuiver Wetenschappelijk Onderzoek (ZWO).

*Permanent address: Institute of Nuclear Research, Shanghai, Peoples Republic of China.

[1]S. L. Ruby and D. I. Bolef, Phys. Rev. Lett. **5**, 5 (1960).
[2]J. Mishory and D. I. Bolef, in *Mössbauer Effect Methodology*, edited by I. Gruverman (Plenum, New York, 1968), Vol. IV, p. 13.
[3]G. L. Zhang, E. H. du Marchie van Voorthuysen, and H. de Waard, Phys. Lett. **91A**, 417 (1982).
[4]G. J. Perlow, Phys. Rev. Lett. **40**, 896 (1978).
[5]J. E. Monahan and G. J. Perlow, Phys. Rev. A **20**, 1499 (1979).
[6]P. Helistö, T. Katila, W. Potzel, and K. Riski, Phys. Lett. **85A**, 177 (1981).
[7]E. H. du Marchie van Voorthuysen, G. L. Zhang, and H. de Waard, Hyperfine Interact. **15/16**, 1025 (1983).
[8]V. A. Burov, V. A. Krasil'nikov, and O. Yu. Sukharevskaya, Zh. Eksp. Teor. Fiz. **43**, 1184 (1962) [Sov. Phys.—JETP **16**, 837 (1963)].
[9]G. J. Perlow, W. Potzel, R. M. Kash, and H. de Waard, J.

Phys. (Paris) Colloq. **35**, C6-197 (1974).
[10]A. R. Mkrtchyan, G. A. Arutyunyan, A. R. Arakelyan, and R. G. Gabrielyan, Phys. Status Solidi **92**, 23 (1979).
[11]T. E. Cranshaw and P. Reivari, Proc. Phys. Soc., London **90**, 1059 (1967).
[12]L. Pfeiffer, N. D. Heiman, and J. C. Walker, Phys. Rev. B **6**, 74 (1972).
[13]A. Abragam, *L'Effet Mössbauer* (Gordon and Breach, New York, 1964), p. 22.
[14]J. M. Ziman, *Electrons and Phonons* (Clarendon, Oxford, 1960), p. 157.
[15]A. Gupta, Phys. Rev. B **24**, 2362 (1981).
[16]G. N. Watson, *Theory of Bessel Functions* (Cambridge University, Cambridge, England, 1966), p. 395.
[17]N. I. Ognjanov and L. T. Tsankov, J. Phys. **44**, 859 (1983).
[18]S. O. Rice, Bell Sys. Tech. J. **3** (1944).
[19]J. G. Stevens, Hyperfine Interact. **13**, 221 (1983).
[20]Made by Dr. A. R. Arends, Noorderdwarsstraat 1, Groningen.
[21]L. T. Tsankov, Bulg. J. Phys. **5**, 149 (1978); **6**, 163 (1979); Nucl. Instrum. Methods **160**, 195 (1979).